The Variabilities of Convective Precipitation and Large-scale Precipitation in Southern China under Global Warming

han zhang
Lanzhou University https://orcid.org/0000-0001-9468-5271
Junhu Zhao
Laboratory for Climate Studies
Bicheng Huang
Lanzhou University
Naihui Zang
Lanzhou University
Jie Yang
Lanzhou University
Feng Guolin (fenggl@cma.gov.cn)
Lanzhou University

Research Article

Keywords: Global Warming, troposphere, influenced

Posted Date: November 9th, 2021

DOI: https://doi.org/10.21203/rs.3.rs-948834/v1

The Variabilities of Convective Precipitation and Large-scale Precipitation in Southern China under Global Warming

Han Zhang[1], Junhu Zhao[2], Bicheng Huang[1], Naihui Zang[1], Jie Yang[3], and Guolin Feng[1,2,4*]

[1]College of Atmospheric Sciences, Lanzhou University, Lanzhou 730000.
[2]Laboratory for Climate Studies, National Climate Research Center, China Meteorological Administration, Beijing 100081.
[3]Jiangsu Climate Center, Jiangsu Meteorological Bureau, Nanjing 210008.
[4]Southern Marine Science and Engineering Guangdong Laboratory, Zhuhai 519000.

* Corresponding authors address:
Prof. Guolin Feng
College of Atmospheric Sciences,
Lanzhou University,
Lanzhou 730000, P. R. China
E-mail: fenggl@cma.gov.cn

Other author Email address:
Mr. Han Zhang: zhangh2019@lzu.edu.cn
Dr. Junhu Zhao: zhaojh@cma.gov.cn
Mr. Bicheng Huang: huangbch18@lzu.edu.cn
Mr. Naihui Zang: zangnh18@lzu.edu.cn
Dr. Jie Yang: yangjie19840827@163.com

ABSTRACT

In this paper, the spatial and temporal characteristics of convective precipitation (CP) and large-scale precipitation (LSP) in southern China during 1980-2020 are analyzed using monthly mean precipitation data from MERRA-2. In addition, the possible effects of relative humidity on CP and LSP are explored. The results indicate the following. (1) The LSP dominates the proportion of total precipitation (TP). Both LSP and CP are more prevalent in the south and less prevalent in the north, but there is a difference in the regions of their maximum centers. (2) Significant interannual and seasonal variations are observed in precipitation. TP and LSP tended to be higher than average after the 1990s, while for the CP, a negative trend has dominated the past years with considerable fluctuation. There are obvious increasing trends for TP and LSP, with area-averaged linear trends of 7.0 mm/year and 8.9 mm/year, respectively, while that of CP is -1.9 mm/year. The increasing trends of LSP are mainly contributed by the precipitation of summer and autumn. (3) The variations of LSP are affected by relative humidity in the troposphere, while CP is only influenced by the changes in relative humidity due to air temperature or specific humidity. The trend of relative humidity is -0.32%/decade, mainly due to rising temperature in the troposphere. (4) Changes in specific humidity caused by temperature or specific humidity alone act on large-scale precipitation through both interannual and interdecadal processes, causing large-scale precipitation to increase. And the convective precipitation is mainly affected by the interdecadal processes.

1 Introduction

The IPCC Fifth Assessment Report revealed that the annual average precipitation in the mid-high latitudes of the Northern Hemisphere has increased since the 1950s under the influence of global warming (Hartmann et al. 2013). The precipitation trend exhibits distinct spatial signatures, but there are no certain long-term trends in the tropical regions or on land at the global scale ((Hartmann et al. 2013; Wan et al. 2013). Trends of extreme precipitation can differ from the implied trends of average precipitation. Global extreme precipitation has increased significantly in many regions due to global warming with a growth rate of approximately 7%/°C; this is termed the Clausius–Clapeyron rate (Trenberth et al. 2007; Hartmann et al. 2013; Seneviratne et al. 2012; Zhang and Zhou 2019; Trenberth et al. 2003; Kharin et al. 2013; Westra et al. 2013). Extreme precipitation causes disasters such as floods, droughts, and landslides, and changes in extreme precipitation can affect society more directly than can variations in most other meteorological elements that can be observed (Allan and Soden 2008). In the absence of significant changes in average precipitation on land at the global scale, extreme precipitation has increased markedly, indicating that the nature of precipitation has been significantly modified. Thus, it is necessary to further understand the variety of different types of precipitation and the responses of precipitation to global warming.

Precipitation can be divided into two components, namely, convective and stratiform precipitation (Houze 1997); this division is one of the most important ways to study precipitation. Since these two types of precipitation are related to cloud physics and have important effects on general atmospheric circulation, it is beneficial to study the effects of the controlling factors on precipitation (Zipser et al.,1977; Leary and Houze 1979). The characteristics of convective and stratiform precipitation have been studied for several years. Sui (2007) noted that stratiform precipitation exhibits weaker radar echoes, smaller vertical velocities and larger extents than convective precipitation, and the ratio of ice water to liquid water is greater than 1 in the former (Sui et al. 2007). Using three-hourly synoptic observations to separate the two types of precipitation in Germany from 1997 to 2004, Berg (2013) reported that the 99th percentile of stratiform precipitation increases with temperature at a rate of approximately 7%/°C, while the rate of increase in the 99th percentile of convective precipitation (CP) almost doubles. Additionally, the relative contribution of CP to total precipitation (TP) can increase with temperature. All of these findings reveal that CP reacts more sensitively to changes in temperature than stratiform precipitation (Berg et al. 2013); in this context, the influence of CP on TP, especially extreme precipitation, will increase with global warming.

Ruiz et al. (2013) analyzed the characteristics of convective and stratiform precipitation along the Eastern Iberian Peninsula during 1998-2008. The results show that both convective and stratiform precipitation have interannual and seasonal variations, and a significant increasing trend of stratiform precipitation leads to a positive trend of annual TP. Seasonal differences in the contributions of different types of precipitation to TP were also reported (Tremblay 2005; Ruiz-Leo et al. 2013). Rulfová (2013) disaggregated the precipitation in the Czech Republic from 1982 to 2010 based on cloud forms and synoptic observations and pointed out that compared with annual stratiform precipitation, CP has larger fluctuations and is the main contributor to the increasing trend of regional precipitation in the Czech Republic (Rulfová and Kyselý 2013). Fu et al. (2016) showed that the intensities of CP and stratiform precipitation in the eastern part of northern China exhibited a significant decreasing trend from 2002 to 2012; conversely, the frequency of CP in the eastern region of southern China had a significant increasing trend (Fu et al. 2016). It is evident that there are considerable regional differences in convective and stratiform precipitation throughout China. Using

TRMM data, Hu et al. (2011) and Liu et al. (2010) indicated that the CP rate in southern China is much larger than the stratiform precipitation rate, but both of them increase gradually as the East Asian summer monsoon advances ((Hu et al. 2011; Liu et al. 2013).

Based on the above studies, it is clear that the characteristics of convective and stratiform precipitation and their contributions to the long-term trend of precipitation vary in both space and time. It is therefore necessary to investigate the annual and seasonal characteristics of both types of precipitation in China under the context of a changing climate. Some studies have been performed on convective and stratiform precipitation in China, but most of them focused on intra-annual characteristics. The time series employed to discuss the trend of precipitation are generally short and limited to satellite data. However, reanalysis data can generally span 40 years or more. Precipitation in reanalysis datasets originates from two distinct parameterization schemes: CP is generated by the convection scheme, which represents convection at spatial scales smaller than the grid box (subgrid), while large-scale precipitation (LSP) is captured by the cloud scheme representing the formation and dissipation of clouds, and the LSP due to changes in atmospheric quantities (such as pressure, temperature and moisture) is predicted directly at spatial scales of the grid box or larger (Dai 2006). According to previous studies, we can adopt a simplified assumption, that is, that the subgrid precipitation (large-scale precipitation) in reanalysis data corresponds to the convective precipitation (stratiform precipitation) in the real atmosphere and that TP is the sum of CP and LSP (Rulfová et al. 2017). Although the scale division of the two types of precipitation is not entirely clear in the real atmosphere, it can often be considered that their overlapping parts can compensate for each other (Kyselý et al. 2015).

Influenced by the East Asian monsoon system and the South Asian monsoon system, the amount of precipitation that falls over southern China is immense, and the seasonal changes in this precipitation are obvious (Seneviratne et al. 2012; Yali et al. 2013). Under the background of global warming, a trend of concurrent droughts and floods has been observed with an increase in the frequency of disasters (Weijing et al. 2016, 2015), all of which exhibit multiscale variability (Huang et al. 2012; Zhang 2015; Si et al. 2016). Therefore, it is crucial to fill the existing research gaps and further improve climate forecasts to study the characteristics of CP and LSP in southern China.

In this study, the spatial-temporal variabilities of annual and seasonal CP and LSP as well as the possible effects of relative humidity (RH), specific humidity (SH) and air temperature (T) on CP and LSP are analyzed in southern China during the period 1980–2020 using atmospheric reanalysis data. The remainder of this paper is structured as follows. After a description of the data and methodology in Section 2, the spatial-temporal characteristics of annual precipitation are presented in Section 3.1, while the spatial-temporal characteristics of seasonal precipitation are shown in Section 3.2. The possible effects of relative humidity, specific humidity and air temperature on precipitation are reported in Section 3.3, and Section 4 presents the conclusions and a discussion of the results.

2 Data and methodology

2.1 Ground observed data

The diurnal observed meteorological data used in this study, including precipitation, are from the daily meteorological data records (V3.0) acquired at 2374 stations in China from January 1951 to December 2019 provided by the National Meteorological Information Center of the China Meteorological Administration. In this study, we have extracted data from 840 observation stations in

southern China (17–30° N, 105–123° E) between 1980 and 2020 (the distribution of these stations is shown in Fig. S1).

2.2 Reanalysis data

In recent years, atmospheric reanalysis data have been produced by several meteorological agencies using assimilation technology. These reanalysis data have high spatial and temporal resolutions, and generally, as the whole world is covered by these data, climate systems around the globe can be analyzed (Tianbao et al. 2010). Recent studies on reanalyses have indeed found that no reanalysis data have an absolutely outstanding ability to predict precipitation, as the applicability of reanalysis data is prone to change in both space and time (Reichle et al. 2017b; Wang et al. 2017). It is necessary to select the most suitable reanalysis data according to the research purpose and area.

The Modern-Era Retrospective Analysis for Research and Applications, version 2 (MERRA-2), is a global atmospheric reanalysis dataset produced by NASA's GMAO (Global Modeling and Assimilation Office); compared with the original MERRA reanalysis, the spatial and temporal resolutions of MERRA-2 are improved, the latest satellite data are added, and the hydrological cycle is improved (Gelaro et al. 2017; Reichle et al. 2017a). MERRA-2 uses observation-based precipitation data as forcing for the land surface parameterization, and the bias corrected precipitation is contained in products (Reichle et al. 2017a). Chen (2019) shows that the precipitation of China is best represented by MERRA-2 than other reanalysis data because the precipitation of MERRA-2 was bias corrected using observed precipitation (Chen et al. 2019). The comparisons we have made between several reanalysis data and observation-based total precipitation do agree with the previous study (Fig. S1 and Fig. S2). Therefore, the precipitation estimates, including total precipitation, convective precipitation and large-scale precipitation, given by MERRA-2 will be used in this paper. To further show the possible causes of the characteristics of TP, LSP and CP, air temperature, relative humidity and specific humidity at 24 levels (1000, 975, 950, 925, 900, 875, 850, 825, 800, 775, 750, 725, 700, 650, 600, 550, 500, 450, 400, 350, 300, 250, 200 and 150 hPa) of MERRA-2 are also used.

2.3 Methodology

2.3.1 Calculation of the average temperature, average specific humidity and average relative humidity in troposphere

The past studies have reported that the troposphere plays an important role in the study of precipitation, it provides a essential feedback mechanism for precipitation (Wu et al. 2015). Thus, it is more suitable to use T, RH and SH data of the troposphere than their surface or lower troposphere data to study the changes of LSP and CP. In this study, the mass-weighted mean method was used to calculate the troposphere average of T, RH and SH (Wu et al. 2015), and there we defined the troposphere ranging from the surface to 150hPa (LIU et al. 2012):

$$e_{ave} = \sum_{Ps}^{150} \mathrm{e}\Delta P \,/\, \sum_{p_s}^{150} \Delta P. \quad (1)$$

where e is the expression for the quantity to be averaged.

Area-averaged quantities are calculated by weighted average method using the cosine of the latitudes as the weights. Linear trend and linear correlation analysis methods are also used in the paper.

2.3.2 Calculation of relative humidity

$$RH = \frac{\mathrm{e}}{e_s} \times 100\%. \quad (2)$$

Where RH is the relative humidity, e and e_s is the actual vapor pressure (hPa) and saturation vapor pressure (hPa), respectively.

$$e_s = 6.1078\, exp\left[\frac{17.2693882(T-273.16)}{T-35.86}\right]. \quad (3)$$

Where T is the temperature (units: K).

$$e = \frac{qPR_v}{[R_d+(R_v-R_d)q]}. \quad (4)$$

Where q is the specific humidity (units: kg kg^{-1}), p is the pressure (units: hPa), R_v is the specific gas constant of water vapor (units: J kg^{-1} K^{-1}), and R_d is the specific gas constant of dry air (units: J kg^{-1} K^{-1}).

3 Results

3.1 Spatial and temporal characteristics of annual precipitation

LSP is usually weak and correlated with long-lived events due to changes in atmospheric quantities in models. CP generally exhibits a shorter duration and greater intensity caused by the strong ascension of local convection under unstable stratification (Tremblay 2005). Thus, there are differences in the precipitation growth mechanism and cloud physical characteristics between the two types of precipitation (Ruiting et al. 2004; Arakawa 2004; Rulfová and Kyselý 2013; Berg et al. 2013). In addition, it is also important to interpret the different atmospheric responses of the two types of precipitation.

Fig. 1 shows the spatial distributions of the different types of annual mean precipitation in southern China (1980-2020) obtained from MERRA-2. Regarding the amount of precipitation, in southern China, the annual LSP is larger than the annual CP. The CP in most areas is below 800 mm, while the LSP is above 800 mm. The two maximum centers of TP (Fig. 1a) correspond to the centers of LSP (Fig. 1c) and CP (Fig. 1b) respectively. The South China and Jiangnan are high-precipitation areas, for the former, the TP and CP exceed 1600 mm and 800 mm, while for the latter, the TP and LSP exceed 1600 mm and 1200 mm, respectively. According to Fig. 1b, the spatial distribution of CP is significantly different from that of LSP, showing a pattern of gradually decreasing from the south to the north.

The general feature of precipitation in southern China is that the amount of LSP exceeds that of CP, consistent with previous studies (Peng and Yu 2010). The proportion of CP gradually decreases from south to north with values ranging from 20% to 30% in Jiangnan and the Southwest China to more than 30% in South China, especially in southern South China, where the proportion is more than 50%. Thus, the magnitudes of the two types of precipitation are comparable in southern South China.

The temporal evolution of different types of precipitation also differs significantly. The linear trend coefficient and time series of the annual area-averaged precipitation (CP, LSP and TP) over southern China (22°–30°N, 105°–122°E) from 1980 to 2020 are given in Fig. 2. The trend of TP in most parts of southern China is positive and is significant (with a confidence level above 95%, the threshold value is 0.31) in some areas (Fig. 2a). The trend coefficient of LSP shows a spatial pattern characterized by positive values in most of the southern China; the trend coefficient ranges from 0.4 to 0.6 in most parts (Fig. 2b) with a confidence level of 95%, expect the western of the South China. The trend of CP is negative and significant (with a confidence level above 95%) in Southwest China (Fig.

2c). As previous studies have shown, these precipitation trends have obvious spatial differences (D and Y 2009; Zhang and Zhou 2019; Weijing et al. 2015).

For the regional average precipitation, the correlation coefficient between TP and LSP is 0.91 (Table 1), indicating a strong correlation, as they show consistent interannual and interdecadal characteristics. With respect to their long-term changes, the TP and LSP show increasing trends, approximately 70 mm/10 a and 89 mm/10 a (exceeding the 99% confidence level), respectively (Fig. 2d and Fig. 2e). The annual CP has decreasing trend of approximately -19mm/10 a during 1980-2020 (Fig. 2f). The trends of the different types of precipitation are caused by changes in their frequency and intensity throughout China, but their changes are not completely consistent in space and time (Fu et al. 2016; Han et al. 2016). The 9-year moving averages of the different precipitation anomalies show interdecadal characteristics. The interdecadal changes in TP (Fig. 2d) are consistent with those in LSP (Fig. 2e). The precipitation anomalies were below average until the late 1990s and then above average from the late 1990s to the present. the variation of CP is clearly different from that of TP and LSP. the CP was below average from the 1980s to the early 1990s and then above average until the 2010s. In the last decade, CP has generally been below average (Figure 2f).

In summary, there is a positive trend of TP in most parts of southern China, which is contributed by LSP. The time series of the TP anomalies are consistent with those of LSP, showing a "negative-positive" pattern from the 1980s to 2010s, whereas CP was below average before 1992/1993 and in recent years.

3.2 Spatial and temporal characteristics of seasonal precipitation

In addition to interannual variability, intra-annual variabilities are also observed in CP and LSP. From the perspective of its temporal and spatial distributions, the monthly TP (Fig. 3a) in southern China remains above 175 mm in summer, and there are clear seasonal differences. After April, the center of the region with the largest TP gradually moves southward and is above 175 mm in Jianghuai and Jiangnan, which is during the meiyu season (from June to July). At the same time, the precipitation center is over South China with values exceeding 225 mm. Then, the precipitation decreases in July and August, and the precipitation center moves southerly (south of 23°N). The temporal and spatial distributions of LSP (Fig. 3b) seem to be different from those of TP. The LSP center in May is mainly located in southern Jiangnan and northern South China, where the monthly mean precipitation is more than 125 mm. After May, CP increases significantly, with the monthly mean precipitation reaching more than 125 mm, and the precipitation center is located over South China. The area begins to expand northward in June and is maintained until August, and then the CP decreases rapidly. Past studies have pointed out that the onset of the South China Sea summer monsoon in late May will gradually affect South China and continue northward. The South China Sea summer monsoon will enhance the instability of stratification, which will lead to an increase in CP (Bin et al., 2006). On the other hand, in summer, especially in August, many typhoons will make landfall along the coast of China, bringing heavy rainfall to eastern China (Shen et al., 2013), which also contributes to the summer CP in South China and Jiangnan. It can be seen that the changes in LSP and CP, as well as their movements in space, correspond to the development of the East Asian monsoon.

Fig. 3d illustrates the intra-annual differences in CP and LSP more clearly. On the one hand, at the same time of year, the relative contribution of CP to TP gradually decreases from south to north, which is quite consistent with the above conclusion. On the other hand, it is found that the contribution of CP

gradually increases from 20% in March and continues to expand northward. From May to September, the contribution of CP in southern South China increases to more than 40% and can reach 60% in summer. The area where CP accounts for more than 30% is the maximum, covering the area south of 30°N. This finding has also been demonstrated by Hu et al (Hu et al., 2011).

Therefore, regarding the different types of annual mean precipitation, LSP is always dominant in southern China. After the onset of the South China Sea summer monsoon in May, both CP and LSP begin to increase, and the proportion of CP begins to increase gradually, reaching a peak in summer. Then, the East Asian summer monsoon weakens in September, and CP also decreases rapidly.

Fig. 4 shows the spatial distributions of the trend coefficients of precipitation in each season from 1980 to 2020.

The TP in spring (Fig. 4a) do not have a significant trend in southern China. Except for some parts in the South China and eastern Jiangnan where the trend coefficient is negative, other areas have a slightly increasing TP trend. Fig. 4b shows decreasing trends of CP in southern China in spring. For the LSP, there are increasing trends along the Yangtze River Basin and the eastern part of southern China, and the trend in the former is statistically significant at 0.05 level (the threshold is 0.31).

The TP in summer (Fig. 4d) shows an increasing trend in most parts of southern China, and this trend is significant in eastern and central Jiangnan and in most parts of South China. The spatial patterns of LSP (Fig. 4f) in summer are similar to that of TP, with significant trend in almost the whole southern China. Fu et al. (2016) also pointed out clear increasing trends in the frequencies of LSP in summer over the southern region of eastern China (Fu et al. 2016). The trend of CP shows a "negative-positive" pattern from the north to the south, the trends pass the significance test (at the 95% confidence level) in eastern Jiangnan. Additionally, in comparison with Fig. 4, the spatial trend patterns of CP and LSP in summer are very similar to those over the whole year. Therefore, it can be considered that the annual trends of the different types of precipitation are mainly contributed by summer precipitation.

The characteristics of precipitation in autumn are depicted in Fig. 4. There is an increasing trend in southern China for TP, and the trends in parts of South China and parts of eastern Southwest China pass the significance test (at the 95% confidence level). The spatial distributions of the trends of LSP (Fig. 4i) in autumn agree well with those in summer. Compared with the corresponding areas in summer, the areas where the LSP show a significant trend in autumn are decreased, while the areas of CP showing a negative trend are increased.

The TP in winter (Fig. 4j) decreases in most parts of South China (Lin and Juan 2011), while there is a positive trend (significant at the 95% confidence level) in eastern Jiangnan. CP (Fig. 4k) shows a distribution of positive values in the east and negative values in the west of southern China. The LSP in winter (Fig. 4L) shows a weak decreasing trend in Southwest China, central and western Jiangnan, and parts of South China, while the increasing trends in eastern Jiangnan pass the significance test at the 95% confidence level.

There are also significant differences in the interannual variations of precipitation in each season and throughout the whole year. Fig. 5 shows the interannual time series of precipitation in different seasons. With regard to the precipitation amount, the amount of LSP in spring is much more than that of CP, generally above 400 mm, while most of the CP was below 200 mm (Fig. 5a). From the perspective of long-term trends, the linear trend coefficients of TP, LSP and CP are 0.12, 0.29, and -0.30, respectively, in spring (Table 2), were not significant. In addition, the correlation coefficients

between TP and the LSP and CP are 0.89 and 0.46, respectively (Table 1), which indicates that the trends of LSP and TP in spring are more consistent because the main sources of spring precipitation in southern China are the spring persistent rains and the first rainy season in South China, which are mainly related to the thermal difference between the land and the sea, the influence of topographic forcing, and the existence of westerlies; the large-scale ascension of condensation precipitation is dominant (GuoXiong Wu and Wan 2006; Rugui et al. 1983).

In summer (Fig. 5b), CP dominates the proportion of TP. LSP is generally above 200 mm, and CP is generally above 300 mm. Since the 1980s, the summertime fluctuations of CP and LSP have continued to increase. The trend coefficients of TP, LSP and CP are 0.53, 0.68 and -0.12, respectively (Table 2), among which TP and LSP are significant at the 99% confidence level (the threshold is 0.40).

According to Fig. 5c, the LSP in autumn has obvious interannual fluctuations, with the minimum being less than 100 mm (1992) and the maximum being greater than 300 mm (2016), and is generally above 150 mm, while the CP is basically below 100 mm. LSP gradually decreased before the end of the 1990s and then increased until the present day, but such changes in CP are not evident. The trend coefficients of TP, LSP and CP in autumn are 0.28, 0.40, and -0.29, respectively (Table 2), and the trend of LSP is significant at the 99% confidence level.

The precipitation in winter (Fig. 5d) is the lowest in the whole year, and the amount of CP is almost negligible. Compared with those in the other seasons, the interannual fluctuations of the LSP in winter are severe, with the minimum being about 100 mm and the maximum being greater than 250 mm (2016). Winter is the only season in which the TP show decreasing trends among the four seasons, the decreasing trend is contributed by CP (Table 2). Past studies have proven that the first mode of winter precipitation in southern China exhibits significant interdecadal changes and has experienced a negative phase transition since the 21st century, while the second mode of winter precipitation in southern China has decreased in recent years (Lin and Juan 2011).

In summary, the positive trend of TP is mainly the result of the effect of LSP while CP contributes to the negative trend, and the pattern of TP depends on LSP. From a seasonal perspective, the increasing trend in LSP and CP is significantly the largest (in all four seasons) and significant in summer, while a weak, insignificant positive trend exists in spring. Thus, the annual trend of TP is mainly contributed by the increase of LSP during summer. In addition, the decreasing trend of CP was weakest in summer, to which sufficient moisture may have contributed.

3.3 The possible effects of relative humidity, specific humidity and air temperature

The spatial and temporal characteristics of CP and LSP are discussed above. There is no doubt that the features of precipitation are affected by a variety of climate systems and meteorological elements; undoubtedly, both temperature and moisture are important factors (Xiaoxia et al. 2008; Zhang and Zhou 2019), especially under the background of global warming. Past studies have shown that the distribution of relative humidity can influence cloud distribution and climate feedbacks to some extent, and thus the type of precipitation (Zelinka et al., 2013), as evidenced by the model's ability to simulate convective and large-scale precipitation in correlation with its accuracy for relative humidity (Jing YANG et al., 2021). Here, we use the mass-weighted averaged RH, T and SH data of MERRA-2 for further research.

According to the Clausius–Clapeyron equation and the saturation vapor pressure formula, the RH is influenced by temperature and moisture (Allen and Ingram 2002; Wu et al. 2015). If the SH was

constant, RH would increase (decrease) when the temperature decrease (increase), for the decreasing (increasing) saturation vapor pressure. When the temperature is unchanged, vapour pressure would increase (decrease) due to increasing (decreasing) SH, leading to the increasing (decreasing) of RH. The spatial and temporal characteristics of the mass-weighted mean troposphere air temperature and specific humidity variation in southern China (22°–30°N, 105°–122°E) from 1980 to 2020 are shown in Fig. 6. The linear trend of T and SH was 0.27K/decade and 0.067g·kg^{-1}/decade, respectively, which reached the 99% significance level. The relative humidity was calculated for three cases to compare the effect of air temperature and specific humidity on relative humidity (Zhou et al. 2020). In the first case, when both specific humidity and air temperature vary with time, the RH_{Tq} can be calculated. The second case is when specific humidity is constant (the value in 1980 was used) and air temperature varies with time, we can obtain RH_t. Similarly, when air temperature remains unchanged, but the specific humidity changed, the RH_q is obtained.

Fig. 7a shows that there is a decreasing trend in the relative humidity in the troposphere with a rate of -0.32%/decade. A decreasing trend was also found for RH_{Tq} with a rate of -0.24%/decade, and the time series of RH_{Tq} is consistent with that of RH (Fig. 7b). The correlation coefficient was 0.99, passing the 99.9% significance level. RH_T decreases significantly at a rate of -0.9%/decade (Fig. 7c), much higher than RH and RH_{Tq}, while RHq increases significantly at a rate of 0.64%/decade (Fig. 7d). In addition, the linear correlation coefficient between RH and T is -0.17, while between RH and SH is 0.47 (Not given in the paper). Referring to the Fig. 8b and Fig. 8c, the maximum center of correlation coefficients between RH and CP, LSP concentrate on South China and eastern Jiangnan, which coincide with that between RH and SH. For the correlation between T and RH, there are negative values that are not significant over the most parts of southern China (Fig. 8e). In addition, the correlation coefficient after a nine-year sliding average shows that the correlation coefficient between RH and T reached -0.55, while the correlation coefficient between RH and SH was 0.01 (Not given in the paper). Which show that the decreasing long-term trend of RH is mainly contributed by air temperature, while the interannual variabilities of RH agree well with that of SH.

According to the above conclusion, the increasing air temperature contribute to the decrease of RH, and the increasing SH leads to an increase in RH. The increasing SH weaken the decreasing trend of RH; thus, the rate of RH is smaller than that of RH_T. So how does the relative humidity in the troposphere under different scenarios affect different types of precipitation? Nine-year Lanczos filter is applied to separate the interannual and interdecadal components. The interannual and interdecadal correlations between relative humidity in different scenarios and different types of precipitation are shown in Table 3.

As shown in Table 3, there are significant positive interannual correlations between RH and TP, and LSP with correlation coefficients of 0.42, 0.36, respectively, and insignificant positive interannual correlations with CP. Interannual (-0.54, -0.60), interdecadal negative correlations (-0.84, -0.75) between RHt and TP, LSP are significant, proving that RH_T affects TP and LSP through both interannual and interdecadal variation, as does RH_q (Table 3). In contrast, CP was mainly influenced by the interdecadal variability of RHt and RHq with correlation coefficients of -0.6 and -0.28, respectively (Table 3). However, the joint effect of temperature and specific humidity was not significant, and the correlation coefficients of RH_{Tq} and CP were 0.19 and 0.15, respectively.

Fig. 9 summarized the possible effects of relative humidity, specific humidity and air temperature on convective precipitation, large-scale precipitation and total precipitation. The rising of the temperature in the troposphere results in the decrease of relative humidity, and an increase in specific humidity leads to an increase in relative humidity. Changes in specific humidity caused by temperature or specific humidity alone act on large-scale precipitation through both interannual and interdecadal processes, causing large-scale precipitation to increase. For the decrease of convective precipitation, it is mainly the interdecadal processes that play a role. In addition, the increase of relative humidity caused by specific humidity can weaken the decrease of relative humidity as a result of the increase of temperature in the troposphere. There is a positive trend of total precipitation as the sum of convective precipitation and large-scale precipitation.

4 Conclusion and discussion

In the past, studies on CP and LSP in China focused on their summer characteristics (Han et al. 2016; Fu et al. 2016). In this study, we revealed the annual and seasonal variations in LSP and CP in southern China using MERRA-2 reanalysis data. Subsequently, we analyzed the correlations between the relative humidity and the two types of precipitation throughout southern China under the background of global warming, and further, explored the possible influences of troposphere specific humidity and air temperature.

The main findings can be summarized as follows:

1. The annual CP in southern China is generally characterized by a meridional distribution; the CP gradually decreases from south to north, which results in an increasing proportion of CP from north to south, with the maximum value being less than 50% in South China. The amount of LSP is greater than that of CP in southern China, and the maximum value of LSP is in the northern part of South China and Jiangnan.
2. After the 1990s, the annual mean TP and LSP were mainly above average, a positive trend of them has dominated the past decade with considerable fluctuation. For the long-term trend, we can conclude that the TP and LSP in most areas of southern China have an obvious increasing trend, with area-averaged linear trends of 7.0 mm/year and 8.9 mm/year, respectively. While the decreasing trend of CP exists in the western Jiangnan with area-averaged linear trends of -1.9 mm/year. The increasing trends of LSP are mainly contributed by the precipitation of summer and autumn. By contrast, the decreasing trend of CP is the weakest in summer.
3. The variations of LSP are affected by relative humidity in the troposphere, while CP is only influenced by the changes in relative humidity due to air temperature or specific humidity. The trend of relative humidity caused by an increase in temperature alone was −0.90%/decade, whereas the trend in relative humidity caused by an increase in specific humidity alone was 0.64%/decade. The trend of relative humidity is -0.32%/decade, as the result of the increase of temperature in the troposphere, and the rising specific humidity slow down the decreasing trend of relative humidity. thus, temperature has a more important role in the variation of relative humidity.
4. Although the decreasing long-term trend of RH is mainly contributed by air temperature, the interannual variabilities of RH are depend on that of SH. Changes in specific humidity caused by temperature or specific humidity alone act on large-scale precipitation through

both interannual and interdecadal processes, causing large-scale precipitation to increase. And the convective precipitation is mainly affected by the interdecadal processes. As results, the TP displays an increasing trend.

In this paper, we find that the LSP is mainly influenced by interannual variation of RH, while the interannual, interdecadal correlation between CP and RH were not significant. As we have known that LSP is mainly affected by large-scale ascension, whereas CP is more related to the instability of stratification (Ruiting et al. 2004). Thus, the annual correlation between LSP and meteorological elements could be the result of air-sea interaction, and the specific mechanism of the changes of CP may need to add additional elements about energy (Allen and Ingram 2002).

References

Allan RP, Soden BJ (2008) Atmospheric warming and the amplification of precipitation extremes. Science 321:1481–1484. https://doi.org/10.1126/science.1160787

Allen MR, Ingram WJ (2002) Constraints on future changes in climate and the hydrologic cycle. Nature 419:228-232.

Arakawa A (2004) The cumulus parameterization problem: Past, Present, and Future. J Clim 17: 2493–2525. https://doi.org/10.1175/1520-0442(2004)017<2493:RATCPP>2.0.CO;2

Berg P, Moseley C, Haerter JO (2013) Strong increase in convective precipitation in response to higher temperatures. Nat Geosci 6:181–185. https://doi.org/10.1038/ngeo1731

Chen S, Gan TY, Tan X, Shao D, Zhu J (2019) Assessment of CFSR, ERA-Interim, JRA-55, MERRA-2, NCEP-2 reanalysis data for drought analysis over China. Clim Dyn 53:737–757. https://doi.org/10.1007/s00382-018-04611-1

D C, Y D (2009) Characteristics of Northwest China rainfall intensity in recent 50 years. Chinese J Atmos Sci (in Chinese) 33:923–935.

Dai A (2006) Precipitation characteristics in eighteen coupled climate models. J Clim 19:4605–4630. https://doi.org/10.1175/JCLI3884.1

Fu Y, Chen F, Liu G, Yang Y, Yuan R, Li R, Liu Q, Wang Y, Zhong L, Sun L (2016) Recent Trends of Summer Convective and Stratiform Precipitation in Mid-Eastern China. Sci Rep 6:1–8. https://doi.org/10.1038/srep33044

Gelaro R, McCarty W, Suárez MJ, Todling R, Molod A et al (2017) The modern-era retrospective analysis for research and applications, version 2 (MERRA-2). J Clim 30:5419–5454. https://doi.org/10.1175/JCLI-D-16-0758.1

Wan RJ, Wu GX, (2006) Study on the climatic genesis mechanism of Spring Rain in South China. Sci CHINA Ser D Earth Sci (in Chinese) 36:936–950.

Han X, Xue H, Zhao C, Lu D (2016) The roles of convective and stratiform precipitation in the observed precipitation trends in Northwest China during 1961-2000. Atmos Res 169:139–146. https://doi.org/10.1016/j.atmosres.2015.10.001

Hartmann DL, Klein Tank et al (2013) Observations: Atmosphere and surface, in: Climate Change 2013: The Physical Science Basis: Working Group I Contribution to the Fifth Assessment Report of the Intergovernmental Panel on Climate Change. Cambridge University Press, pp 159–254. https://doi.org/10.1017/CBO9781107415324.008

Hu L, Li YD, Song Y, Deng DF (2011) Seasonal variability in tropical and subtropical convective and stratiform precipitation of the East Asian monsoon. Sci China Earth Sci (in Chinese) 54:1595–1603. https://doi.org/10.1007/s11430-011-4225-y

Huang R, Chen J, Wang L, Lin Z (2012) Characteristics, processes, and causes of the spatio-temporal variabilities of the East Asian monsoon system. Adv Atmos Sci 29:910–942. https://doi.org/10.1007/s00376-012-2015-x

Jing YANG, Sicheng HE, Qing BAO (2021) Convective/Large-scale Rainfall Partitions of Tropical Heavy Precipitation in CMIP6 Atmospheric Models. Advances in Atmospheric Sciences 38:1020-1027.

Kharin VV, Zwiers FW, Zhang X, Wehner M (2013) Changes in temperature and precipitation extremes in the CMIP5 ensemble. Clim. Change 119:345–357. https://doi.org/10.1007/s10584-013-0705-8

Kyselý J, Rulfová Z, Farda A, Hanel M (2015) Convective and stratiform precipitation characteristics in an ensemble of regional climate model simulations. Clim Dyn 46:227–243.

https://doi.org/10.1007/s00382-015-2580-7
Leary CA, RA Houze Jr (1979) The structure and evolution of convection in a tropical cloud cluster. J Atmos Sci 36:437–457.
Lin W, Juan F (2011) Two Major Modes of the Wintertime Precipitation over China. Chinese J Atmos Sci (in Chinese) 35:1105–1116.
LIU H, Zhi-gang W, Hong W, Zheng-chao L, Chao W (2012) Characterstics of Tropopause Height over China in Recent 51 Years. PLATEAU Meteorol (in Chinese) 31:351–358.
Liu P, Li CY, Wang Y, Fu YF (2013) Climatic characteristics of convective and stratiform precipitation over the Tropical and Subtropical areas as derived from TRMM PR. Sci China Earth Sci 56:375–385. https://doi.org/10.1007/s11430-012-4474-4
Peng LIU, Yu FU (2010) Climatic Characteristics of Summer Convective and Stratiform Precipitation in Southern China Based on Measurements by TRMM Precipitation Radar. Chinese J Atmos Sci (in Chinese) 34:802–814.
Reichle RH, Draper CS, Liu Q, Girotto M, Mahanama SPP, Koster RD, De Lannoy, GJM (2017a) Assessment of MERRA-2 land surface hydrology estimates. J Clim 30:2937–2960. https://doi.org/10.1175/JCLI-D-16-0720.1
Reichle RH, Liu Q, Koster RD, Draper CS, Mahanama SPP, Partyka GS (2017b) Land Surface Precipitation in MERRA-2. J Clim 30:1643–1664. https://doi.org/10.1175/JCLI-D-16-0570.1
Rugui S, Quanzhen T, Yingying L (1983) The circulation change in lower and upper troposphere in lower latitudes and the rainfall during the pre-typhoon rain-season. Proc Symp Summer Monsoon South East Asia. People's Press Yunnan Prov (in Chinese) 10–19.
Ruiting Z, Qingcun Z, Ming Z (2004) A Numerical Simulation of Monsoon and the Correlation Between Monsoon and Westerlies. CHINESE J Atmos Sci (in Chinese) 28:7–22.
Ruiz-Leo AM, Hernández E, Queralt S, Maqueda G (2013) Convective and stratiform precipitation trends in the Spanish Mediterranean coast. Atmos Res 119:46–55. https://doi.org/10.1016/j.atmosres.2011.07.019
Rulfová Z, Beranová R, Kyselý J (2017) Climate change scenarios of convective and large-scale precipitation in the Czech Republic based on EURO-CORDEX data. Int J Climatol 37:2451–2465. https://doi.org/10.1002/joc.4857
Rulfová Z, Kyselý J (2013) Disaggregating convective and stratiform precipitation from station weather data. Atmos Res 134:100–115. https://doi.org/10.1016/j.atmosres.2013.07.015
Seneviratne S, Nicholls N, Easterling D et al (2012). Changes in climate extremes and their impacts on the natural physical environment. https://doi.org/10.1017/CBO9781139177245.006
Si D, Hu ZZ, Kumar A, Jha B, Peng P, Wang W, Han R (2016) Is the interdecadal variation of the summer rainfall over eastern China associated with SST? Clim Dyn 46:135–146. https://doi.org/10.1007/s00382-015-2574-5
Sui CH, Tsay CT, Li X (2007). Convective-stratiform rainfall separation by cloud content. J Geophys Res Atmos 112:1–9. https://doi.org/10.1029/2006JD008082
Tianbao Z, Fu C, Jian K, Guo W (2010) Research status and progress of global atmospheric reanalysis data. Adv Earth Sci 25:242–254.
Tremblay A (2005) The stratiform and convective components of surface precipitation. J Atmos Sci 62:1513–1528. https://doi.org/10.1175/JAS3411.1
Trenberth K, Jones P, Ambenje P et al (2007) Observations: surface and atmospheric climate change. Chapter 3, in: Climate Change. pp 235–336.

Trenberth KE, Dai A, Rasmussen RM, Parsons DB (2003) The changing character of precipitation. Bull Am Meteorol Soc 84:1205-1218. https://doi.org/10.1175/BAMS-84-9-1205

Wan H, Zhang X, Zwiers FW, Shiogama H (2013) Effect of data coverage on the estimation of mean and variability of precipitation at global and regional scales. J Geophys Res Atmos 118:534–546. https://doi.org/10.1002/jgrd.50118

Wang G, Wang D, Trenberth KE, Erfanian A, Yu M, Bosilovich MG, Parr DT (2017) The peak structure and future changes of the relationships between extreme precipitation and temperature. Nat Clim Chang 7:268–274. https://doi.org/10.1038/nclimate3239

Weijing L, Jinging Z, Yanling S, Jingpeng L, Yu L, Yuyang S, Jingxin L (2015) Changes in Spatio-Temporal Distribution of Drought/Flood Disaster in Southern China Under Global Climate Warming. Meteorol Mon (in Chinese) 41:261–271.

Weijing L, Ruonan Z, Chenghu S, Hongchang R, Jingpeng L, Jinqing Z, Xiang L (2016) Recent Research Advances on the Interannual Variations of Drought/Flood in South China and Associated Causes. J Appl Meteorol Sci (in Chinese) 27:577–591.

Westra S, Alexander L V, Zwiers FW (2013) Global increasing trends in annual maximum daily precipitation. J Clim 26:3904–3918. https://doi.org/10.1175/JCLI-D-12-00502.1

Wu J, Zhang L, Zhao D, Tang J (2015) Impacts of warming and water vapor content on the decrease in light rain days during the warm season over eastern China. Clim Dyn 45:1841–1857. https://doi.org/10.1007/s00382-014-2438-4

Xiaoxia Z, Yihui D, Panxing W (2008) Moisture transpotr in Asian summer monsoon region and its relationship with summer precipitation in China. Acta Meteorol Sin (in Chinese) 66:59–70.

Yali L, Hui W, Renhe Z, Weimiao Q, Zhengzhao L (2013) Comparison of Rainfall Characteristics and Convective Properties of Monsoon Precipitation Systems over South China and the Yangtze and Huai River Basin. J Clim 26:110–132. https://doi.org/10.1175/JCLI-D-12-00100.1

Zelinka MD, Klein SA, Taylor KE, Andrews T, Webb MJ, Gregory JM, Forster PM (2013) Contributions of different cloud types to feedbacks and rapid adjustments in CMIP5. J Climate 26:5007−5027. https://doi.org/10.1175/JCLI-D-12-00555.1.

Zhang RH (2015) Natural and human-induced changes in summer climate over the East Asian monsoon region in the last half century: A review. Adv Clim Chang Res 6:131–140. https://doi.org/10.1016/j.accre.2015.09.009

Zhang W, Zhou T (2019) Significant increases in extreme precipitation and the associations with global warming over the global land monsoon regions. J Clim 32:8465–8488. https://doi.org/10.1175/jcli-d-18-0662.1

Zhou J, Zhi R, Li Y, Zhao J, Xiang B, Wu Y, Feng G (2020) Possible causes of the significant decrease in the number of summer days with light rain in the east of southwestern China. Atmos Res 236:104804. https://doi.org/10.1016/j.atmosres.2019.104804

Zipser EJ (1977) Mesoscale and convective-scale downdrafts as distinct components of squall-line circulation. Mon Wea Rev 105:1568–1589.

Declarations

Acknowledgments

The authors thanks Dr. Zhao Junhu for the helpful comments on the original manuscript. The daily precipitation data were obtained from the CMA at http://data.cma.cn/. The relative humidity, specific humidity, and temperature data were obtained from https://disc.gsfc.nasa.gov/datasets?keywords=merra2&page=1.

Funding Statement

This study was jointly supported by the National Natural Science Foundation of China (NSFC) [grant number 42130610, 42075017, 41875096, 41875093 and]; the National Key Research and Development Program of China [grant numbers 2017YFC1502303 and 2018YFA0606301].

Conflict of Interest

The authors declare that they have no known competing financial interests or personal relationships that could have appeared to influence the work reported in this paper.

Availability of data and material

The MERRA2 Reanalysis datasets generated during and/or analysed during the current study are available from the corresponding author on reasonable request. The observed daily precipitation data for 2,374 stations that are available from the National Weather Information Center of the China Meteorological Administration.

Code availability

The code analysed during the current study are available from the corresponding author on reasonable request.

Author's contribution

All authors contributed to the study conception and design.

Conceptualization: Han Zhang, Junhu Zhao, Guolin Feng; Methodology: Han Zhang, Junhu Zhao, Bicheng Huang, Naihui Zang; Formal analysis and investigation: Han Zhang, Junhu Zhao, Jie Yang; Writing: Han Zhang.

Ethics approval (Not applicable)

Consent to participate (Not applicable)

Consent for publication (Not applicable)

Figures and tables

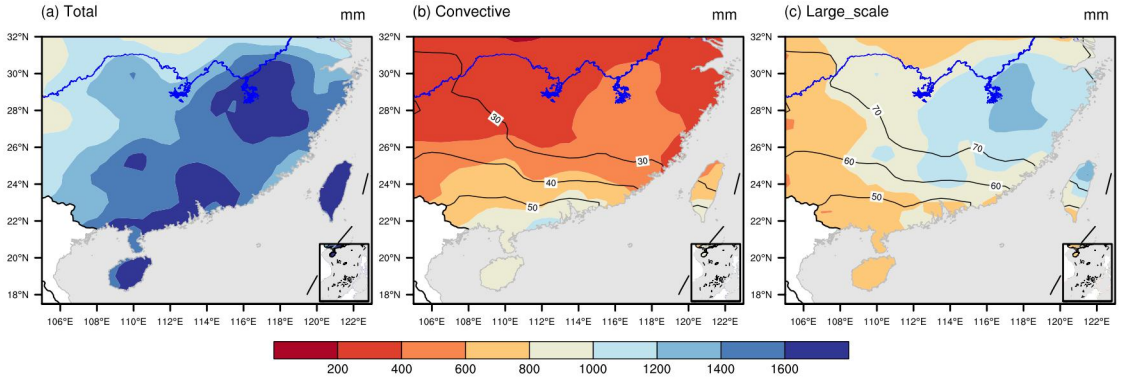

Fig. 1 Spatial distributions of the annual mean (a) total precipitation, (b) convective precipitation and (c) large-scale precipitation from 1980 to 2020 over southern China (units: mm). Contours in (b) and (c) are the percentage distribution of the convective and large-scale precipitation

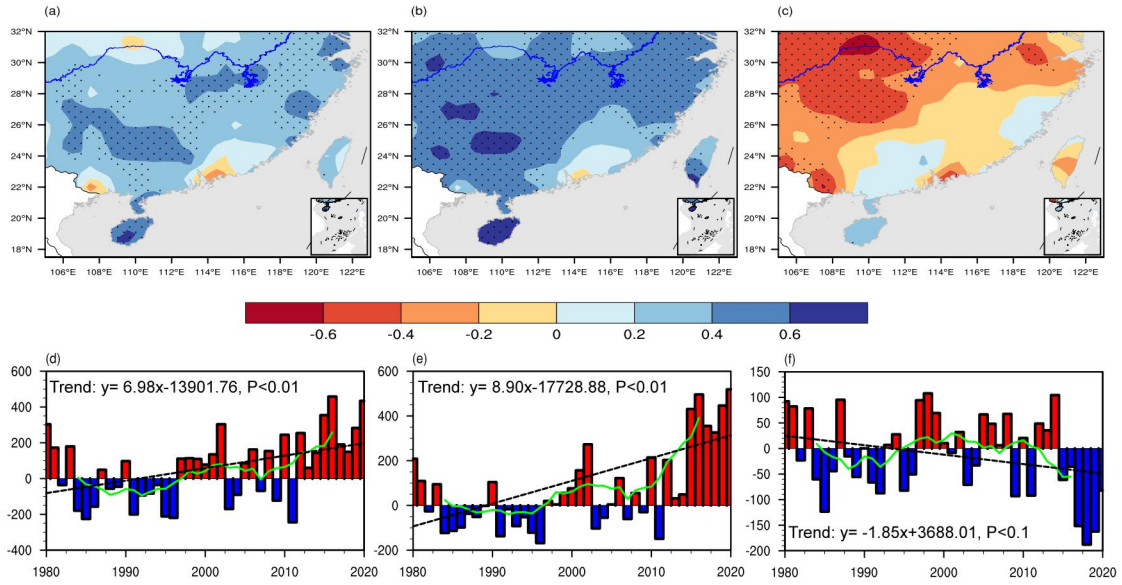

Fig. 2 Spatial distributions of the linear trend coefficients of (a) total precipitation, (b) large-scale precipitation, and (c) convective precipitation from 1980 to 2020. The black dots denote the areas where the trend is statistically significant at the 95% confidence level. (d)-(f) are the time series of the total precipitation, large-scale precipitation and convective precipitation average anomalies over southern China (22°–30°N, 105°–122°E), respectively. The linear trends of precipitation are shown as the black dash lines, and the green curve denotes the nine-year running deviation (unit: mm/year)

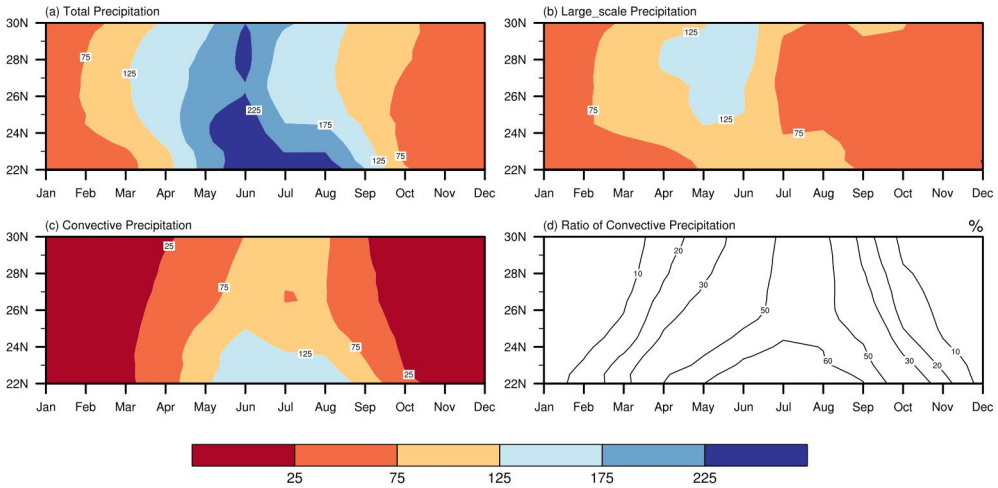

Fig. 3 Zonal mean precipitation for the mean annual (a) total, (b) large-scale, and (c) convective precipitation from 1980 to 2018; (d) Zonal mean contribution of mean annual convective precipitation to total precipitation from 1980 to 2018

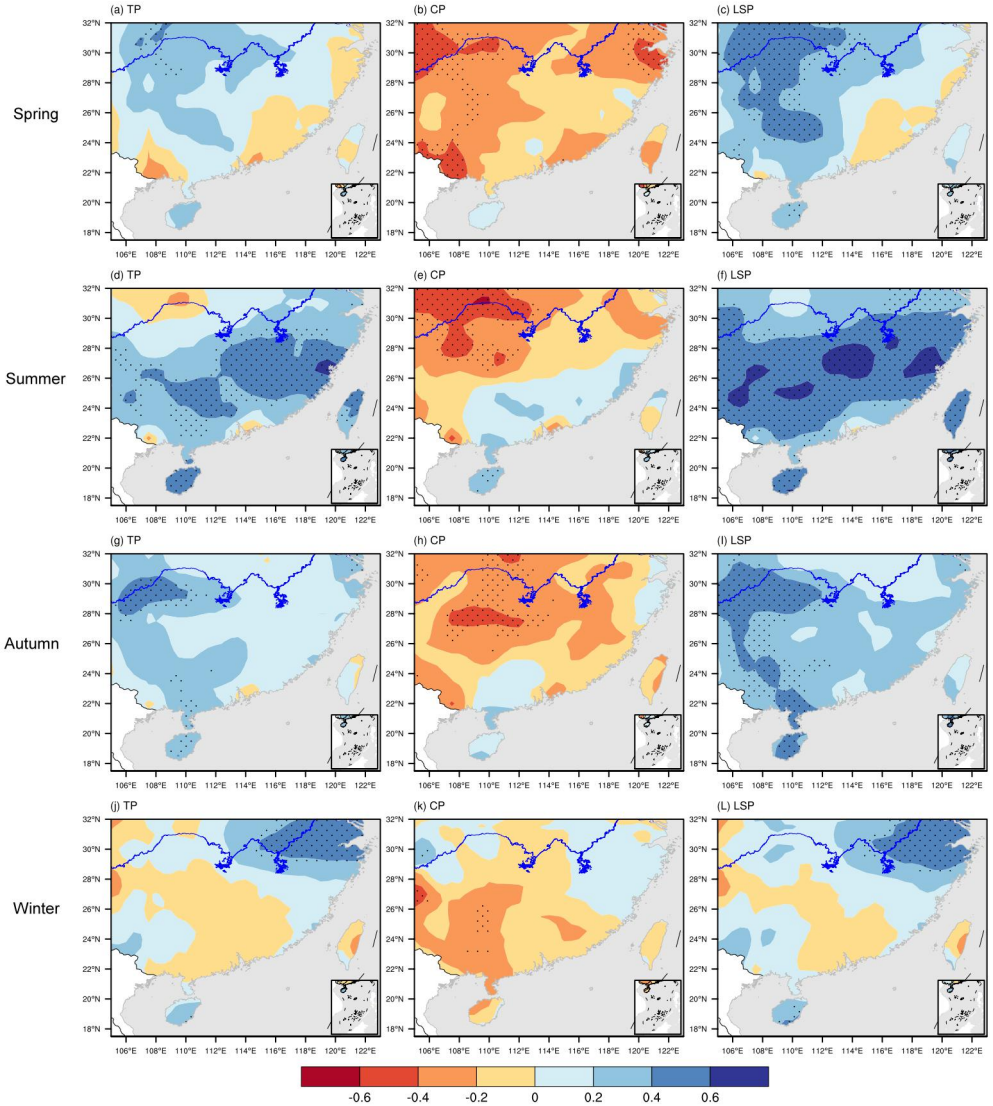

Fig. 4 Same as Fig. 2(a) to (c) but for each season: (a) to (c) spring, (d) to (f) summer, (g) to (I) autumn, and (j) to (L) winter

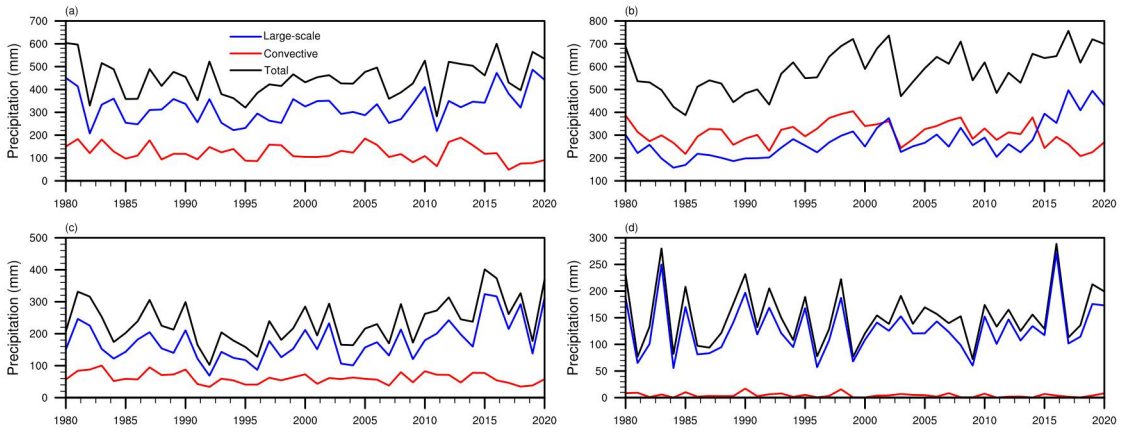

Fig. 5 Time series of the mean seasonal total (black line), large-scale (blue line), and convective precipitation (red line) from 1980 to 2018 over southern China (22°–30°N, 105°–122°E) for (a) spring, (b) summer, (c) autumn, and (d) winter (unit: mm)

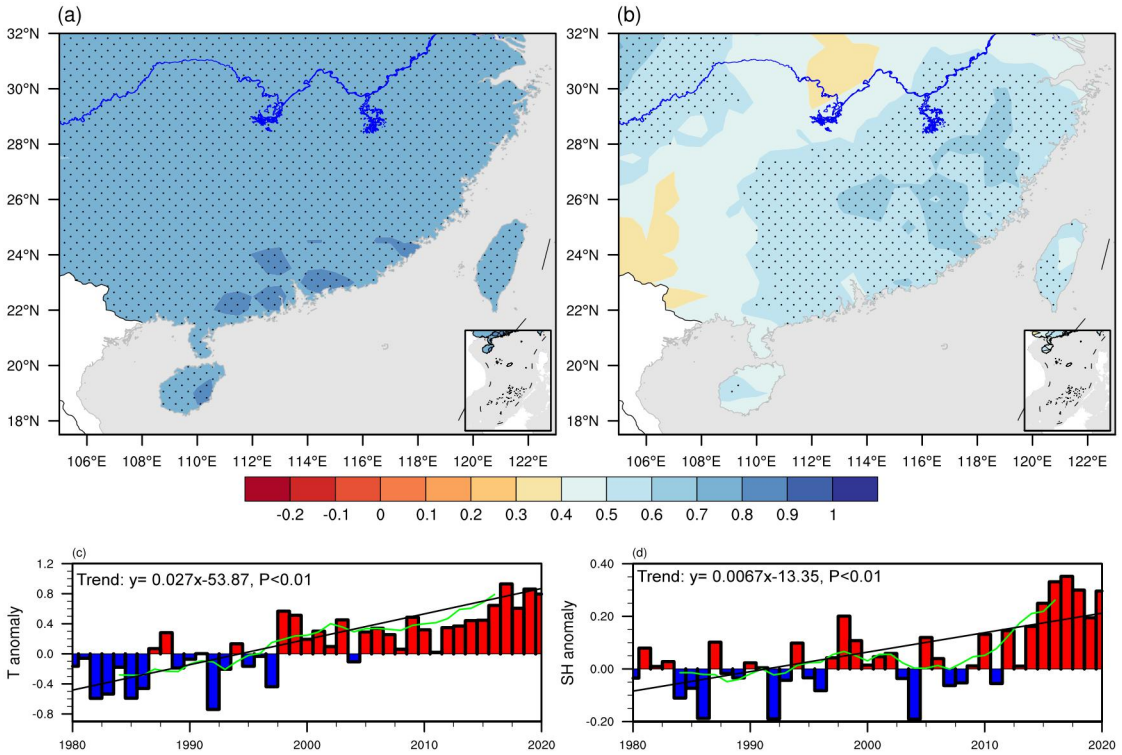

Fig. 6 Same as Fig. 2, but (a) and (c) for air temperature (unit: K/year) while (b) and (d) for specific humidity ($g \cdot kg^{-1}$/year) in the troposphere

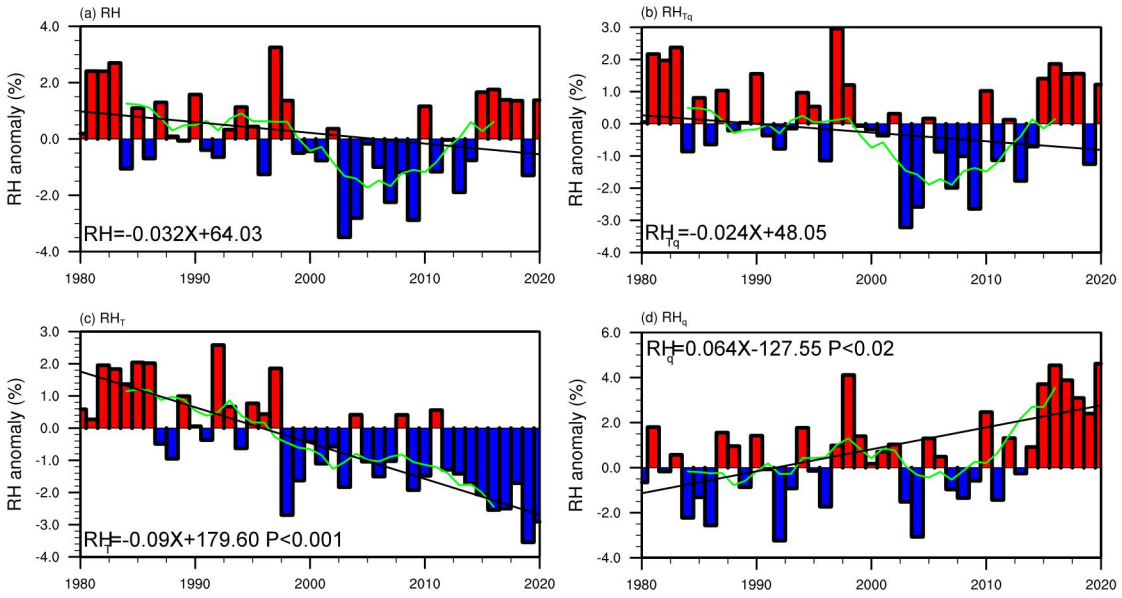

Fig. 7 Time series of relative humidity in the troposphere in the southern China during 1979–2020. (a) Relative humidity, (b) relative humidity caused by temperature and specific humidity (RH_{Tq}), (c) relative humidity caused by the temperature only (RH_T) and (d) relative humidity caused by specific humidity only (RH_q) (units: %/year)

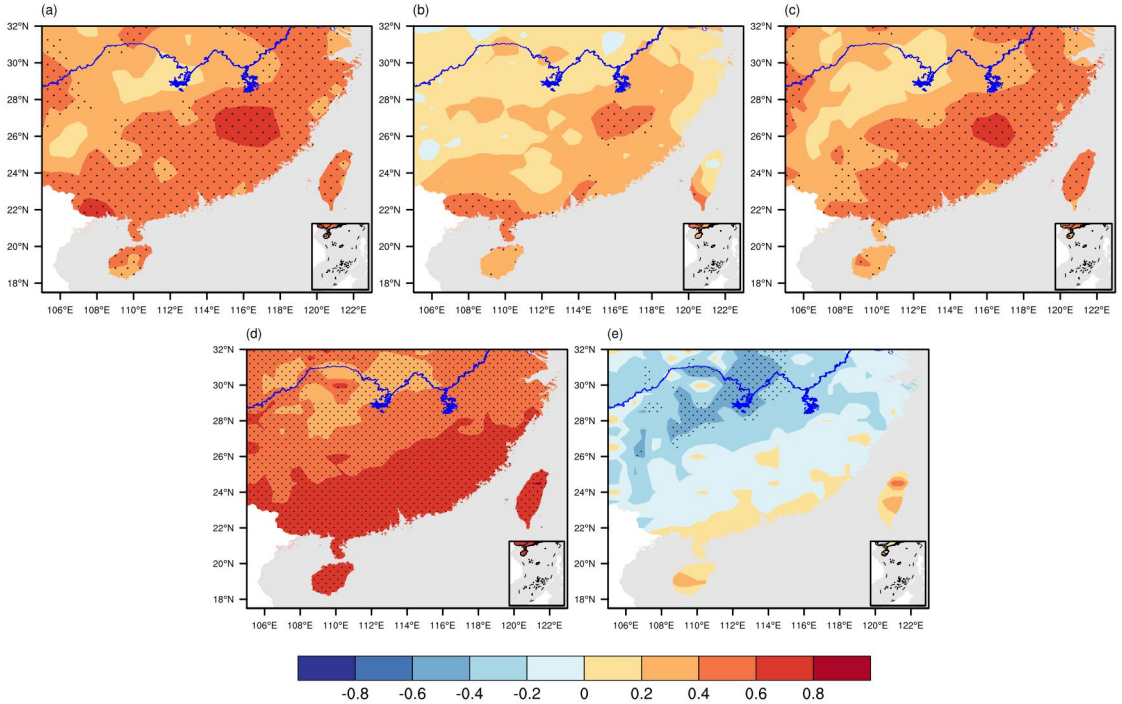

Fig. 8 Spatial distributions of the correlations coefficients between the relative humidity and (a) total precipitation, (b) convective precipitation, (c) large-scale precipitation, (d) specific humidity and (e) air temperture from 1980 to 2020. The black dots denote the areas where the correlation is statistically significant at the 95% confidence level

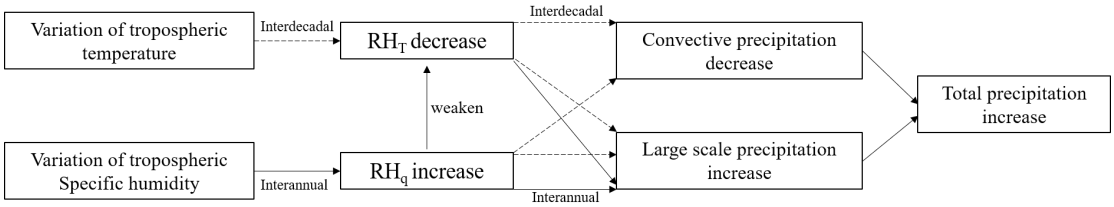

Fig. 9 Summary of the possible effects on the variations of convective precipitation, large scale precipitation and total precipitation in southern China. Dashed arrows indicate interdecadal effects and solid arrows indicate interannual effects

Table 1 Correlation coefficients between different types of precipitation from 1980 to 2020 over southern China. *(**) denotes trend significant at the 0.05 (0.01) significance level

precipitation	TP	LSP	CP
TP	1		
LSP	0.91**/0.89**/0.85**/0.97**/0.98**	1	
CP	0.27/0.46**/0.49**/0.54**/0.54**	-0.14/0.015/-0.047/0.32*/0.52**	1

Table 2 Linear trends coefficients (and trend magnitudes, units: mm/year) of the different types of annual mean precipitation from 1980 to 2020 over southern China. *(**) denotes trend significant at the 0.05 (0.01) significance level

precipitation	Annual	spring	summer	autumn	winter
TP	0.44*(6.98)	0.12(0.79)	0.53**(4.17)	0.28(1.64)	0.06(0.25)
LSP	0.58**(8.90)	0.29(1.68)	0.68**(4.67)	0.40*(2.07)	0.10(0.40)
CP	-0.28(-1.85)	-0.30(-0.87)	-0.12(-0.50)	-0.29(-0.41)	-0.21(-0.07)

Table 3 The interannual and interdecadal correlation coefficients between precipitation and relative humidity from 1980 to 2020 over southern China

pre	RH		RH$_{Tq}$		RH$_T$		RH$_q$	
	interannual	interdecadal	interannual	interdecadal	interannual	interdecadal	interannual	interdecadal
TP	0.42**	0.024	0.46**	0.075	-0.54**	-0.84**	0.75**	0.74**
LSP	0.36*	-0.0032	0.39*	0.045	-0.60**	-0.75**	0.75**	0.64**
CP	0.20	0.12	0.19	0.15	0.09	-0.60**	0.06	0.59**

Note: *(**) denotes correlation significant at the 0.05 (0.01) significance level

Supplementary Files

This is a list of supplementary files associated with this preprint. Click to download.

- SupplementalFigures.pdf